SPANDIDOS PUBLICATIONS

EXPERIMENTAL AND THERAPEUTIC MEDICINE 19: 172-182, 2020

Effect of fosinopril on the renal cortex protein expression profile of Otsuka Long-Evans Tokushima Fatty rats

ZHIGUO LI[1], YEQIANG LIU[2], HAOJUN ZHANG[3], ZHIJIE PU[4], XUEJING WU[4] and PING LI[3]

[1]Department of Medical Research Center, International Science and Technology Cooperation Base of Geriatric Medicine, North China University of Science and Technology, Tangshan, Hebei 063210; [2]Department of Endocrinology, Kailuan General Hospital, Tangshan, Hebei 063000; [3]Beijing Key Laboratory for Immune-Mediated Inflammatory Diseases, Institute of Clinical Medical Sciences, China-Japan Friendship Hospital, Beijing 100029; [4]Graduate School, North China University of Science and Technology, Tangshan, Hebei 063000, P.R. China

Received November 29, 2018; Accepted August 23, 2019

DOI: 10.3892/etm.2019.8188

Abstract. Angiotensin-converting enzyme inhibitors (ACEIs) can reduce urinary protein excretion and postpone the deterioration of renal function. However, the mechanisms of renal protection are not yet fully understood. To investigate the mechanisms of ACEIs in the treatment of diabetic nephropathy (DN), the present study determined the effects of the ACEI fosinopril (FP) on the profiling of renal cortex protein expression in Otsuka Long-Evans Tokushima Fatty (OLETF) rats using Long-Evans Tokushima Otsuka (LETO) rats as controls. Urinary protein levels at 24 h were examined using the Broadford method. PAS staining was performed to observe renal histopathological changes. The kidney cortices of OLETF, FP-treated OLETF and LETO rats were examined using soluble and insoluble high-resolution subproteomic analysis methodology at age of 36 and 56 weeks. Differentiated proteins were further confirmed using western blotting analysis. The results demonstrated that FP significantly decreased the glomerulosclerosis index and reduced the 24 h urinary protein excretion of OLETF rats. Additionally, 17 proteins significantly changed following FP-treatment. Amongst these proteins, the abundances of the stress-response protein heat shock protein family A member 9 and the antioxidant glutathione peroxidase 3 were particularly increased. These results indicated that FP ameliorated diabetic renal injuries by inhibiting oxidative stress. In conclusion, the differentially expressed proteins may improve our understanding of the mechanism of ACEIs in the OLETF rats.

Correspondence to: Professor Ping Li, Beijing Key Laboratory for Immune-Mediated Inflammatory Diseases, Institute of Clinical Medical Sciences, China-Japan Friendship Hospital, 2 Yinghua East Road, Beijing 100029, P.R. China
E-mail: lp8675@163.com

Key words: proteomics, renal cortex, Otsuka Long-Evans Tokushima Fatty rats, diabetic nephropathy, angiotensin-converting enzyme inhibitors, matrix assisted laser desorption/ionization time-of-flight mass spectrometry

Introduction

Diabetic nephropathy (DN) represents one of the major chronic complications of diabetes, causing a progressive decline in glomerular filtration rate (1). In the process of DN initiation and progression, abnormal activation of the renin angiotensin system (RAS), both locally and systemically, generates functional abnormalities in the vasculature. This leads to endothelial dysfunction and extracellular matrix deposition, contributing to sclerosis, fibrosis and progressive DN (2,3). Angiotensin II is known to cause endothelial damage and dysfunction, which then promotes reactive oxygen species (ROS) production and NF-κB activation, potentiating hypertension-induced injury to the glomerular filtration barrier (4,5). Various studies have demonstrated that angiotensin II is a proinflammatory, pro-oxidant peptide that contributes substantially to kidney tissue injury beyond the hemodynamic influences on vascular tone and intraglomerular pressure (6,7). In turn, angiotensin-converting enzyme inhibitors (ACEIs) can inhibit the generation of angiotensin II, thereby effectively blocking ROS, whilst also reducing blood pressure and urinary protein excretion, delaying the deterioration of renal function. These effects have been confirmed by a large number of experiments, and ACEIs have accordingly been used as basic drugs to treat DN in the clinic (8,9). In particular, fosinopril (FP) has been revealed to have significant benefits in the early stages of DN in clinical trials (10). However, the mechanism of action of ACEIs or FP in mediating renal protection is not yet fully understood.

Previous studies have demonstrated that the pathogenesis of DN is very complex (1,11,12). Notably, one of the best animal models available to study DN is the Otsuka Long-Evans Tokushima Fatty (OLETF) rat (13). OLETF rats can spontaneously develop late-onset hyperphagia, mild obesity, late-onset hyperglycemia, hypertension, dyslipidemia and advanced DN. At 12-20 weeks of age, OLETF rats exhibit mild obesity and hyperinsulinemia. Late-onset hyperglycemia is noted by 18 weeks of age. At 22 weeks of age, OLETF rats develop overt albuminuria and at the age of 54 weeks, advanced renal changes such as macroalbuminuria, nodular lesions, diffuse glomerulosclerosis and tubulointerstitial fibrosis are present,

which is comparable to the symptoms of human DN (14). Long-Evans Tokushima Otsuka (LETO) rats are available as a normal control for OLETF rats, as they carry a similar genetic background but do not spontaneously develop diabetes (15).

Therefore, to investigate the mechanisms of action of ACEIs in the treatment of DN, the present study examined the effects of the ACEI FP on protein expression in the renal cortex of OLETF rat using mass spectrometry-based profiling. By incorporating a research model with a consistent genetic background, the experimental design reduced the difficulty of protein analysis inherent in a natural population with obvious heterogeneity. In addition, kidney cortex proteins were separated into soluble and insoluble protein fractions to further overcome the complexity of the OLETF rat kidney cortex proteome. The results of the current study may elucidate novel concepts regarding the underlying mechanism of FP in DN.

Materials and methods

Animals and experimental design. Four-week-old male LETO rats (n=18; weight, 164±6 g) and age-matched OLETF rats (n=24; weight, 207±19 g) that were provided by the Tokushima Research Institute (Otsuka Pharmaceutical). All rats were housed at 22±3˚C and 50±10% humidity using a 12-h light/dark cycle. All animals were given free access to standard rat chow and water.

Three groups of rats at 12 weeks of age were prepared as follows: i) Non-diabetic LETO rats provided with distilled water (LETO control; n=18); ii) diabetic OLETF rats provided with distilled water (OLETF control; n=12); and iii) OLETF rats administered FP (Monopril; Bristol-Myers Squibb) at 0.833 mg/kg body weight/day (OLETF + FP; n=12). FP was dissolved in distilled water and administered once daily by intragastric administration. At 36 weeks of age, 10 rats from the LETO control group and 7 rats from the other two groups were euthanized with an intraperitoneal injection of pentobarbital (200 mg/kg). The remaining rats in each group (8 LETO controls and 5 from each of the other groups) were sacrificed at 56 weeks of age. After the rats were sacrificed, the kidneys were removed and separated into two pieces for histopathological examination and proteomic analysis. The present study was approved by the Ethics Committee of the China-Japan Friendship Institute of Clinical Medicine (no. ZR05016) and performed in accordance with the Guiding Principles for the Care and Use of Laboratory Animals (16).

MTT assay. An MTT assay was performed to analyze whether FP damaged renal tubular NRK-52E cells (Cell Resource Center of Shanghai Institutes for Biological Science) under normal and high glucose conditions. Cells were seeded into 96-well plates ($2x10^3$ cells/well) in 200 μl culture medium (DMEM (Gibco; Thermo Fisher Scientific, Inc.; cat. no. 31600-034) supplemented with 5% fetal bovine serum (Gibco; Thermo Fisher Scientific, Inc.; 16000-044)) treated with different FP concentrations (0, 0.05, 0.10, 0.20, 0.41, 0.83, 1.66, 3.33, 6.66, 13.32 and 26.65 mg/ml) under normal (5 mM) and high (30 mM) glucose media for 48 h at 37˚C. Following treatment, cells were washed twice with PBS and 20 μl MTT (2 mg/ml) was subsequently added into each well. Cells were further incubated for 4 h at 37˚C, after which DMSO was added into each well to dissolve formazan crystals. Absorption was determined at a wavelength 490 nm using a Bio-Rad 680 microplate reader (Bio-Rad Laboratories, Inc.).

Determination of body weight, blood glucose and urinary protein. The body weights of the rats were measured at 4-week intervals. Blood samples from the tail vein were taken at 4-week intervals and blood glucose levels were measured using a One Touch Ultrablood glucose monitoring system (LifeScan, Inc.). Rats were housed individually in metabolic cages (Suzhou Fengshi Laboratory Animal Equipment Co., Ltd.) for urinary collection for 24 h at 4-week intervals.

Histological examination of the kidney. Sections of kidney tissue were removed and immediately fixed in 10% phosphate buffered formalin solution at room temperature for 24 h and embedded in paraffin for further histological and immunohistochemical analysis. Sections (3 μm) from each sample were cut and stained with periodic acid Schiff's stain for evaluation of the degree of glomerulosclerosis, defined as a thickening of the basement membrane and mesangial expansion from 40 glomeruli in each section at x400 magnification (17). Tubulointerstitial and vascular damage were assessed on periodic acid Schiff-stained paraffin sections at x100 magnification using a similar scoring system (0-4) as previously described (18). The observer was blinded to all tissue samples.

Immunohistochemistry. Kidney injury molecule-1 (KIM-1) immunohistochemical staining was performed to analyze whether FP caused OLETF renal damage. All procedures were performed in accordance with the Elivision™ Plus Two-step System PV-6000 kit protocol (Zymed; Thermo Fisher Scientific, Inc.; cat. no. PV6000). Paraffin sections (3 μm thick) as aforementioned were deparaffinized in xylene and rehydrated in descending alcohol series, after which endogenous enzyme activity was blocked via incubation in 3% hydrogen peroxide for 10 min at room temperature. Antigen retrieval was performed by incubating samples with 0.01 mol/l sodium citrate buffer (pH 6.0) at 115˚C for 1.5 min. Tissue sections were subsequently incubated with primary polyclonal antibodies against KIM-1 (Boster Biological Technology; cat. no. BA35317; 1:100) overnight at 4˚C. After washing with PBS, sections were incubated with secondary antibodies (included in the Dako Elivision™ Plus Two-step System PV-6000 kit; Zymed; Thermo Fisher Scientific, Inc,) for 25 min at 37˚C. The signal was subsequently visualized using the Diaminobenzidine. Following counterstaining with hematoxylin for 15 min at room temperature, positive immunostaining was scored by two blinded experienced pathologists. Immunohistochemistry results were evaluated using an Olympus BX53 upright light microscope and scored by examining 10 random representative fields at a 400x magnification. The staining intensity of each visual field was graded from 0 to 3+, as descried by Zhang (19).

Extraction of renal cortical soluble and insoluble protein fractions. The method of extraction of soluble and insoluble protein was based on a previously described protocol with some modifications (20). Briefly, the renal cortical tissue samples from the LETO, OLETF and OLETF treated with FP

groups were ground into powder in liquid nitrogen individually. Soluble lysis buffer [40 mM Tris, pH 7.5; 1% dithiothreitol; 1% IPG buffer, pH 3-10; and protease inhibitor cocktail (Roche Diagnostics)] were added to dissolve the powder, and the mixture was then centrifuged at 40,000 x g at 4˚C for 30 min to separate the soluble and insoluble fractions. The soluble fraction was further centrifuged at 40,000 x g at 4˚C for 30 min to separate out any remaining insoluble content. The insoluble fraction was washed twice with soluble lysis buffer (details as aforementioned) to wash out any soluble proteins. The insoluble pellet was suspended in insoluble lysis buffer (40 mM Tris, pH 7.5; 7 M urea; 2 M thiourea; 4% CHAPS; 1% dithiothreitol; 1% IPG buffer, pH 3-10; and complete protease inhibitor cocktail) and then subjected to ultrasound homogenization at 5 sec pulsed intervals at 20 kHz for 1 min on ice. The homogenized pellet was then put on ice for 30 min and the solution was spun at 40,000 x g at 14˚C for 30 min to separate out any insoluble content. Protein concentration was determined using the Bradford protein assay on a GeneQuant 1300 spectrometer (GE Healthcare Life Sciences). The protein extracts were stored at -80˚C for subsequent two-dimensional electrophoresis (2-DE) analysis.

2-DE and matrix assisted laser desorption/ionization time-of-flight mass spectrometry (MALDI-TOF MS). Each prepared soluble and insoluble protein was separated by 2-DE individually and the differentially expressed proteins were identified by MALDI-TOF MS using a method described previously (21). In brief, samples of 1.3 mg soluble or insoluble protein were loaded on an immobilized pH gradient gel strip (pH 3-10 NL, 24 cm; GE Healthcare) using the in-gel rehydration mode. Proteins were separated by first dimensional separation (Ettan IPGphor 3 Isoelectric Focusing Unit; GE Healthcare), and 13% total monomer concentration and 3% weight percentage of crosslinker second dimensional separation (Ettan DALT II system; GE Healthcare). The separated protein spots were visualized using colloidal Coomassie blue staining according to the manufacturer's protocol (GE Healthcare), and the resultant images were analyzed using ImageMaster 2D Platinum 6.0 software (GE Healthcare), according to manufacturer's protocol. Statistical analysis was carried out using the t-test and false discovery rate as described by Biron *et al* (22). The differentially expressed protein spots were cut manually from the gels with a stainless-steel scalpel. The in-gel digestion and MALDI-TOF MS of each excised protein spot were performed by the National Center of Biomedical Analysis (Beijing, China).

Database search. The obtained MS data were identified by using the Mascot search engine (www.matrixscience.com/cgi/search_form.pl?FORMVER=2&SEARCH=PMF) according to the specific peptide mass fingerprints (PMF). Identified proteins were further checked for reliability following the criteria by Biron *et al* (22) as follows: i) molecular weight search Score >60 (calculated as -10*Log (P); P<0.05, default threshold); ii) proportion of the theoretical sequence of the protein covered by MS data ≥20%; and iii) compared with theoretical values, a molecular mass variation <30% and isoelectric point variation <2.0. Each identified candidate protein entry was traced to its corresponding official gene name using the Protein Information Resource (Georgetown University Medical Center).

Functional classification of differentially expressed proteins. To obtain an overview of the differentially expressed protein functions of the OLETF rat kidney cortex, the online tool DAVID Bioinformatics Resources 6.7 (https://david-d.ncifcrf.gov/) was used to perform enrichment analysis using gene ontology (GO) terms and KEGG pathways (23). The threshold was set as P<0.05 to explore the overrepresentation of biological terms and signaling pathways.

Western blot analysis. As not all identified proteins had commercial antibodies and due to economic limitations, heat shock protein family A member 9 (Hspa9) and glutathione peroxidase 3 (Gpx3) were selected as representative proteins and examined by western blot analysis to confirm their expression alterations. Protein samples from 2-DE analysis (15 μg) were separated via SDS-PAGE using a 12% polyacrylamide gel and electro-transferred to a nitrocellulose membrane in a Trans-Blot® Semi-dry Electrophoretic Transfer Cell (Bio-Rad Laboratories, Inc.). Nonspecific bands were blocked in TBS-T (25 mM Tris, 150 mM NaCl and 0.05% Tween-20; pH 7.5) containing 5% skimmed milk at room temperature for 1 h. Membranes were subsequently incubated with a primary antibody against Hspa9 (Santa Cruz Biotechnology, Inc.; 1:1,000; cat. no. SC-133137), Gpx3 (Abcam; 1:1,000; cat. no. ab256470) and β-actin (Tianjin Sungene Biotech Co.; 1:5,000; cat. no. KM9001) overnight at 4˚C followed by incubation with an anti-mouse (Jackson ImmunoResearch Laboratories, Inc.; 1:3,000; cat. no. 115-035-003) or anti-rabbit IgG (Jackson, 1:3,000; cat. no. 111-035-003) horseradish peroxidase-conjugated secondary antibodies at room temperature for 1 h. The immunocomplexes were visualized by enhanced chemiluminescence using the Amersham ECL Western Blotting Detection kit (GE Healthcare). The signals were acquired by the chemiDoc™ XR+ molecular imager (Bio-Rad Laboratories, Inc.) and then quantified using Quantity-One 4.31 software (Bio-Rad Laboratories, Inc.).

Statistical analysis. SigmaPlot 12.5 (Systat Software, Inc.) was used to analyze data and determine statistical differences. Each experiment was at independently replicated 3 times and data were presented as the mean ± standard deviation. Data that met the criteria for parametric tests were analyzed by Student's t-test (two groups) or by a one-way ANOVA and a subsequent Bonferroni post-hoc test (more than two groups). Groups of data that failed tests for normality and equal variance were analyzed by the nonparametric Kruskal-Wallis test followed by Dunn's test. P<0.05 was considered to indicate a statistically significant difference.

Results

FP treatment lowers 24-h urinary protein levels in OLETF rats. The body weights of OLETF rats were greater than those of LETO rats between 12 and 48 weeks; however, no significant differences were observed when compared with OLETF rats treated with FP. In addition, at weeks 52 and 56, body

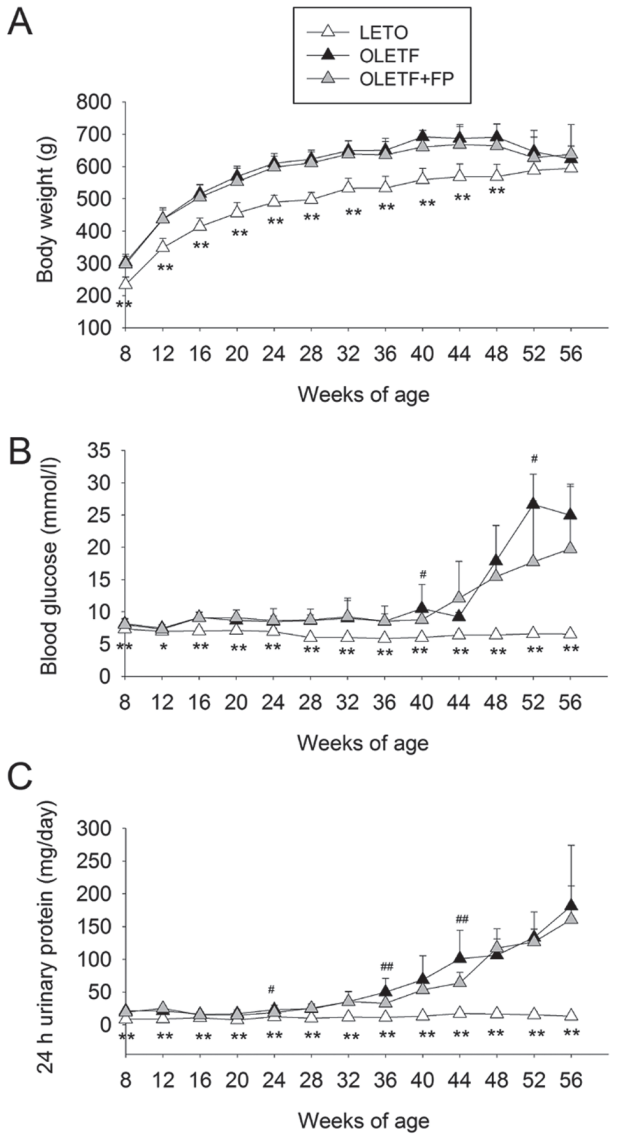

Figure 1. Comparison of LETO, OLETF and FP-treated OLETF rats with respect to (A) body weight, (B) blood glucose level and (C) 24-h urinary protein level over 56 weeks. Data are presented as the mean ± SD. *P<0.05 and **P<0.01 vs. respective OLETF group; $^{\#}$P<0.05 and $^{\#\#}$P<0.01 vs. respective OLETF+FP group. LETO, Long-Evans Tokushima Otsuka; OLETF, Otsuka Long-Evans Tokushima Fatty; FP, fosinopril.

weight did not differ significantly among the groups (Fig. 1A). Blood glucose levels for the LETO control rats did not change throughout the study period. Over the same period of time, age-matched OLETF rat blood glucose levels were statistically higher. The blood glucose levels of OLETF rats treated with FP also increased during the study period, with levels significantly different from those of the OLETF control group at weeks 40 and 52 (Fig. 1B). Urinary protein levels in all OLETF rats gradually and continually increased during the entire study period compared with the levels in the LETO rats, which remained unchanged. OLETF rats treated with FP exhibited significantly lower 24-h urinary protein levels than those exhibited by the OLETF control group at weeks 24, 36 and 44 (Fig. 1C).

FP treatment ameliorates histological kidney changes in OLETF rats. Glomerular lesions in OLETF rats were characterized by hyalinosis, thickening of the basement membrane, mesangial expansion and sclerosis (Fig. 2A). These pathological changes were more severe at 56 weeks of age than at 36 weeks. Interstitial fibrosis in OLETF rats was focal and mild at 36 weeks of age, whereas at 56 weeks of age severe changes occurred that included protein cast, tubular dilation or atrophy and infiltration of inflammatory cells (Fig. 2A). Treatment with FP significantly ameliorated glomerulosclerosis in OLETF rats at both 36 and 56 weeks of age (Fig. 2B), but was unable to attenuate the increase in interstitial fibrosis (Fig. 2C).

Comparative proteomic analysis of renal cortices from untreated and FP-treated OLETF rats. Fig. 3 displays representative 2-DE patterns of soluble and insoluble renal cortex proteins from untreated and FP-treated OLETF rats. Comparison of the protein profiles from the two groups identified that 9 protein spots (S1-S9) were differentially expressed in the soluble subproteome and 10 protein spots (I1-I10) were differentially expressed in the insoluble subproteome (Fig. 4). These protein spots were submitted for MALDI-TOF MS analysis. All protein spots were successfully isolated and their PMF, protein name and related data were obtained in the corresponding database and are listed in Table I. Certain different protein spots were identified as the same protein, likely because of different translational or post-translational modifications leading to changes in physicochemical characteristics during protein expression, resulting in their separation into different protein spots in 2-DE. The differentially expression of Hspa9 and Gpx3 were further validated by western blot analysis. As shown in Fig. 5, the expression levels of Hspa9 and Gpx3 at 56 weeks were similar to those observed in the 2-DE gels. The abundances of the proteins increased significantly in the renal cortex of OLETF rats treated with FP at 56 weeks.

DAVID analysis revealed over-representation of pathways and terms (Table II) in the differentially expressed proteins from this tissue. Specifically, 'glycolysis/gluconeogenesis' was over-represented among the identified KEGG pathways. 'Generation of precursor metabolites', 'energy, glucose metabolic process' and 'oxidation reduction' were over-represented in biological processes. Furthermore, differentially expressed proteins were over-represented in the mitochondrion and soluble fraction. Within these, there was over-representation of molecular functions including 'magnesium ion binding', 'selenium binding' and 'hydro-lyase activity'.

Discussion

DN is a main cause of end-stage renal disease that currently has no effective treatment to block or reverse its pathological process. A number of clinical and basic studies have investigated ACEIs/angiotensin II receptor blockers (24-26) for the treatment of DN to delay the progression of the disease, and these drugs have been recommended by the Kidney Disease Outcomes Quality Initiative as first-line clinical treatments (27). However, studies have identified that ACEIs demonstrate some nephrotoxicity since ACEIs, including FP, may cause an exaggerated or progressive decline in renal function in conditions such as renal-artery stenosis (28,29) and polycystic kidney disease (30), due to their preferential vasodilation of the renal efferent arteriole.

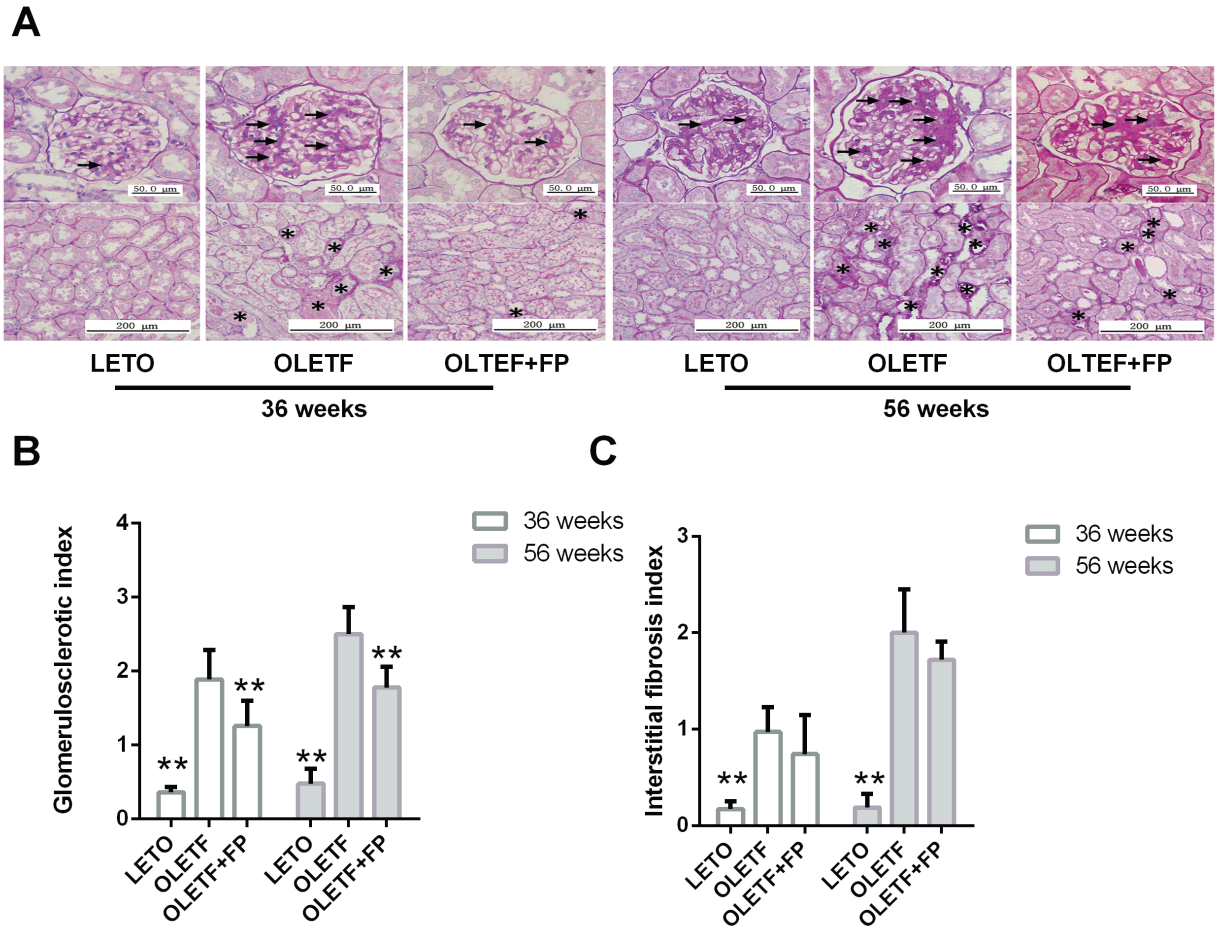

Figure 2. Histologic changes between LETO, OLETF and FP-treated OLETF rat kidneys. (A) Periodic acid-Schiff staining of renal glomeruli and tubules. (B) Glomerulosclerosis index. (C) Interstitial fibrosis index. Data are presented as the mean ± SD. *P<0.05 and **P<0.01 vs. respective OLETF group. LETO, Long-Evans Tokushima Otsuka; OLETF, Otsuka Long-Evans Tokushima Fatty; FP, fosinopril.

The present study determined that the ACEI drug FP reduced the pathological damage to renal tissue in OLETF rats and reduced urinary protein excretion. FP significantly inhibited the expression of KIM-1, an early marker of renal injury in OLETF rats (Fig. S2), indicating that FP exerts good renoprotective effects. *In vitro* experiments also confirmed that FP had a significant effect on the proliferation of NRK-52E cells at 13.32 μg/ml, which was ~119 times the maximum blood concentration in human (112±8 ng/ml; Fig. S1) (31), suggesting that FP improves diabetic kidney injury with no obvious nephrotoxic effects.

In the development of DN, proteinuria not only serves as an important marker for evaluating pathological progression but also participates in the development of renal fibrosis (32). Albumin and other proteins that appear in urine due to abnormal filtration, can interact with the glomerular mesangium and proximal tubule (33), which activates a wide array of intracellular signaling pathways, such as the ERK, NF-κB and protein kinase C pathways (34). This induces fibrotic substances, such as transforming growth factor-β, collagens, C-C motif chemokine 2 and metalloproteinase inhibitor 1 (33,35,36), and ultimately leads to fibrosis and loss of renal function (37). The present results demonstrated that FP alleviated proteinuria in OLETF rats, suggesting that this may have a role in improving diabetic glomerular sclerosis and tubulointerstitial fibrosis. Subsequent experiments investigating the renal cortex proteomics profile in OLETF rats determined that FP treatment resulted in significant changes in the abundance of 17 proteins, including Hspa9 and Gpx3. Bioinformatics analysis indicated that the function of these differentially expressed proteins likely participated in biological processes such as oxidative stress and glucose metabolism. Therefore, FP may have a renoprotective role by increasing the expression of Hspa9 to inhibit oxidative stress, consequently reducing tissue and cell damage.

In the present study, compared with the OLETF control, treatment with FP caused a significant increase in the abundance of the plasma glutathione peroxidase precursor Gpx3. Gpx comprises an important part of the antioxidant mechanism in body (38,39) and is actively expressed in human kidney proximal tubule cells (40). Previous research determined that hyperglycemia induces the overproduction of superoxide by the mitochondrial electron transport chain, leading to an increase in ROS greater than the antioxidant capacity of the body, resulting in cell and tissue damage (12). In addition, high glucose can stimulate 12-lipoxygenasein podocytes,

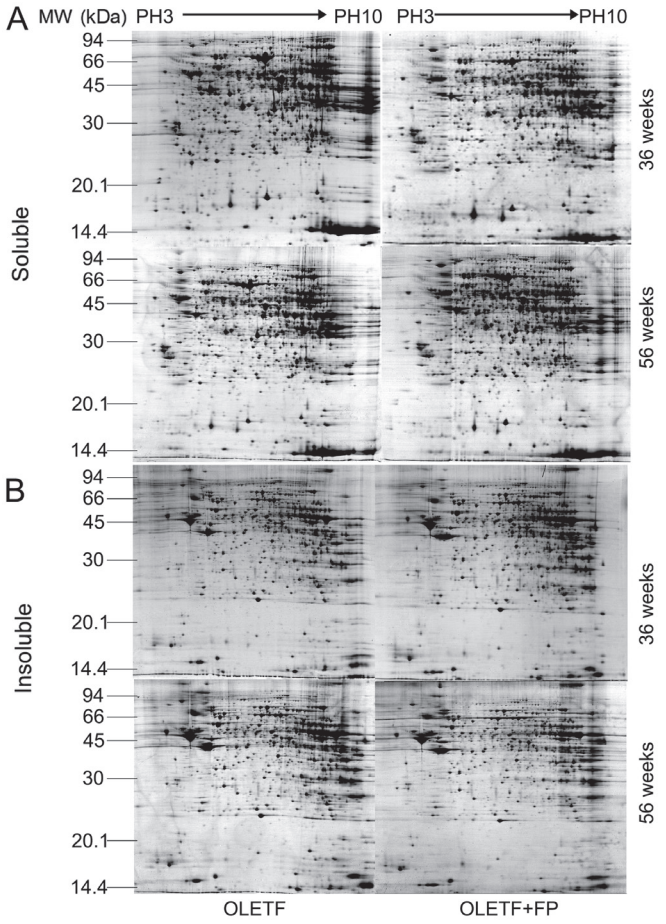

Figure 3. Comparison of (A) soluble and (B) insoluble subproteome 2-DE patterns in OLETF and FP-treated OLETF rat renal cortices. 2-DE, two-dimensional electrophoresis; OLETF, Otsuka Long-Evans Tokushima Fatty; FP, fosinopril.

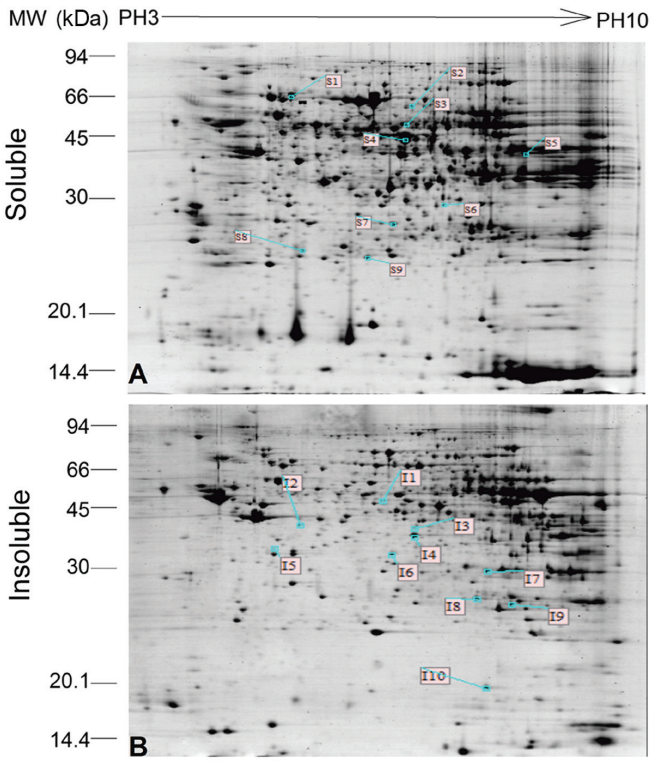

Figure 4. Differentially expressed proteins distribution in the (A) soluble and (B) insoluble subproteome shown by two-dimensional gel electrophoresis analysis.

which also leads to oxidative stress through the generation of superoxide (41). Based on such observations, Brownlee (12) proposed that the overproduction of superoxide was likely to be a common mechanism for the pathogenesis of diabetic complications. Consistent with this, angiotensin II has been shown to induce ROS production and the activation of NF-κB and mitogen activated protein kinase in diabetic glomeruli and mesangial cells (34). As angiotensin II is an important medium of oxidative stress, studies have accordingly begun to explore the use of ACEIs for reducing oxidative stress levels in patients with DN. Notably, these trials have demonstrated that ACEIs and angiotensin II receptor blockers are able to reduce oxidative stress and inflammation in patients with DN and that this effect is independent of the antihypertensive effect (42,43). It has been suggested that the specific mechanism may involve a reduction of oxidative stress-associated damage by blocking the NADPH oxidase pathway (44) by decreasing the elevation in ROS generation induced by platelet-derived growth factor (45). Another potential mechanism might involve attenuating apoptosis and intracellular ROS formation induced by angiotensin II through modulation of the toll like receptor 4/MYD88 innate immune signal transduction adaptor pathway (46). Furthermore, previous studies determined that Gpx3 interacts with podocin, which is used as a marker of podocytes (47,48) and is associated with microalbuminuria in DN (49). Taken together, Gpx3 may serve an important role in the development of DN. In the present study, it was determined that FP treatment increased the Gpx3 precursor concentration in the renal cortex of OLETF rats. These results suggested that FP could inhibit the development of DN by stimulating increased Gpx3 expression.

The results of the present study also indicated that FP affected the expression of Hspa9, which has begun to attract attention regarding its role in the pathogenesis of DN (50). Hspa9 also known as glucose regulated protein 75, mortalin, mitochondria heat shock protein 70 and peptide binding protein 74, is mainly localized in the mitochondria, where it functions as a molecular chaperone, serving a central role in the elaborate translocation system for the efficient import and export of proteins and maintaining the function of the mitochondria (51). Mutations in Hspa9 cause the degeneration of nerve cells and have a role in the pathogenesis of Parkinson's disease (52). Hspa9 binds to p53 protein in the cytoplasm and inhibits its function acting as an anti-apoptotic factor. Consistent with this, Hspa9 is found to be upregulated in many human cancer types, suggesting its association with the occurrence and metastasis of malignant tumors (53). In addition, high levels of Hspa9 expression can protect the cell from a variety of stress-induced damage types, reducing the effects of various physical and chemical factors. For example, it has been shown that Hspa9 overexpression can reduce the damage to cells mediated by glucose deprivation and that the protective effect may be achieved by inhibiting the accumulation of ROS (54). The antioxidant function has also been confirmed by many other studies (55-57), including the normalization of high-glucose-induced

Table I. Effect of fosinopril on the renal cortex protein expression profile of OLETF rats.

Spot no.	GI no.	Protein name	Gene name	Mass	Sequence coverage (%)	MOWSE score	Age, weeks	Protein abundance
S1	gil1000439	grp75	Hspa9	32/48	46	239	36 56	N ↑
S2	gil40254595	Dihydropyrimidinase-related protein 2	Dpysl2	19/57	43	108	36 56	↓ ↓
S3	gil149030730	Selenium binding protein 2	Selenbp1	11/35	35	88	36 56	↓ ↓
S4	gil158186649	α-enolase	Eno1	26/46	66	222	36 56	↓ N
S5	gil40254752	Phosphoglycerate kinase 1	Pgk1	21/33	56	204	36 56	N ↓
S6	gil157823267	S-formylglutathione hydrolase isoform a	Esd	9/39	33	62	36 56	N ↑
S7	gil51491893	Phenazine biosynthesis-like domain-containing protein	Pbld1	10/21	32	126	36 56	↓ ↓
S8	gil6978515	Apolipoprotein A-I preproprotein	Apoa1	14/59	48	83	36 56	N ↑
S9	gil6723180	Plasma glutathione peroxidase precursor	Gpx3	15/21	42	136	36 56	↑ ↑
I1	gil158186649	α-enolase	Eno1	8/16	27	80	36 56	N ↑
I2	gil51036635	Fructose-1, 6-bisphosphatase 1	Fbp1	13/19	33	144	36 56	N ↑
I3	gil170295834	NADH dehydrogenase [ubiquinone] 1 alpha subcomplex subunit 10, mitochondrial precursor	Ndufa10	15/26	31	175	36 56	↑ ↑
I4	gil170295834	NADH dehydrogenase [ubiquinone] 1 alpha subcomplex subunit 10, mitochondrial precursor	Ndufa10	17/24	56	241	36 56	↓ N
I5	gil56090293	Pyruvate Dehydrogenase E1 component subunit beta, mitochondrial precursor	Pdhb	16/33	34	108	36 56	↑ N
I6	gil15100179	Malate dehydrogenase, cytoplasmic isoform Mdh1	Mdh1	10/16	30	128	36 56	N ↑
I7	gil57527204	Electron transfer flavoprotein subunit alpha, mitochondrial precursor	Etfa	20/54	58	168	36 56	N ↓
I8	gil24159081	Chain A, crystal structure analysis of rat enoyl-Coa hydratase in complex with hexadienoyl-Coa	Echs1	21/40	56	158	36 56	N ↓
I9	gil68163417	Acylpyruvase FAHD1, mitochondrial	Fahd1	10/17	32	90	36 56	↓ ↓

Table I. Continued.

Spot no.	GI no.	Protein name	Gene name	Mass	Sequence coverage (%)	MOWSE score	Age, weeks	Protein abundance
I10	gil55926145	Nucleoside diphosphate kinase B	Nme2	8/12	55	102	36 56	N ↓

Spot numbers were defined according to the spot positions in 2-DE gels. GI numbers are a series of digits assigned consecutively by the National Center for Biotechnology Information to each sequence as an identifier. Mass is the number of matched mass values/number of total mass values searched. Sequence coverage was calculated as the percentage of identified sequence to the complete sequence of the matched protein. The MOWSE score of the identified protein was calculated as -10*Log (P), where P is the probability that the observed match is a random event. Changes in renal cortex protein abundance in OLETF rats treated with fosinopril compared with OLETF rats were as displayed on the 2-DE gels. N, no significant change; ↑, increased abundance; ↓, decreased abundance; S, soluble component; I, insoluble component; OLETF, Otsuka Long-Evans Tokushima Fatty; 2-DE, two-dimensional electrophoresis; MOWSE, Molecular Weight Search.

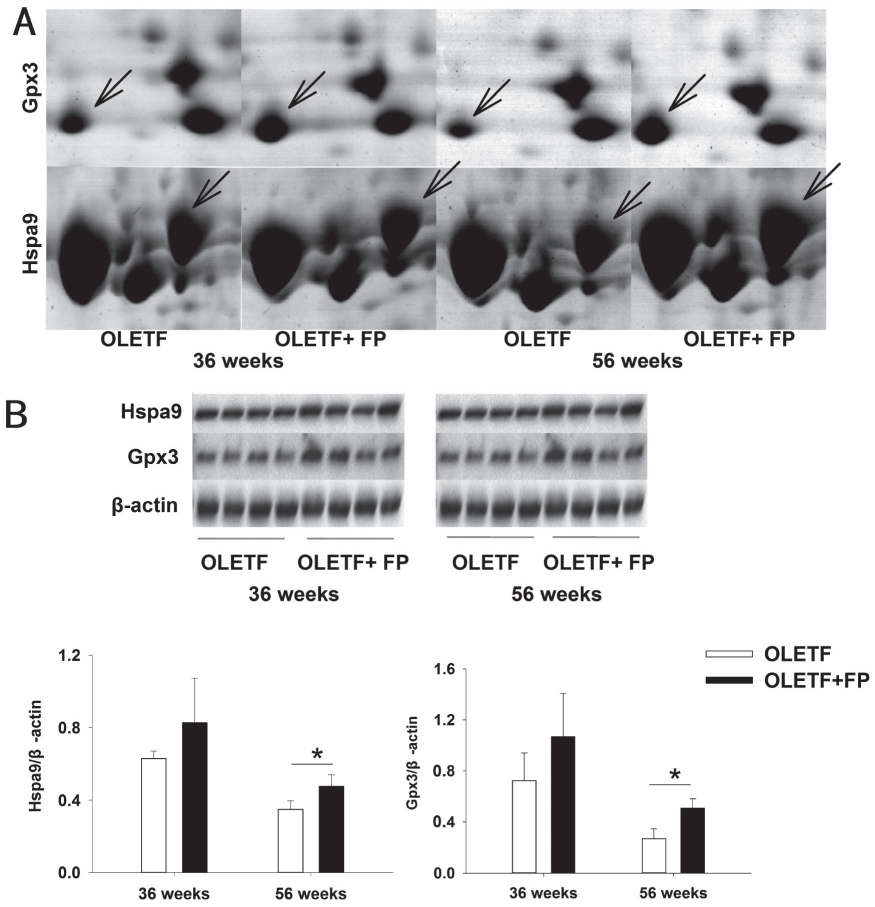

Figure 5. FP treatment increases Gpx3 and Hspa9 expression in OLETF rats. (A) Magnified comparison map of Gpx3 and Hspa9 in the subproteome (B) and western blot analysis of Gpx3 and Hspa9 expression in OLETF and FP-treated OLETF rat renal cortices. Data are presented as the mean ± SD. *P<0.05 with comparisons indicated by lines. Gpx3, glutathione peroxidase 3; Hspa9, heat shock protein family A member 9; OLETF, Otsuka Long-Evans Tokushima Fatty; FP, fosinopril.

enhanced ROS production through the endogenous overexpression of translocase of inner mitochondrial membrane (Tim)44 combined with facilitated import of antioxidative enzymes such as superoxide dismutase and GPx, as Tim44 forms a complex with Hspa9 and Tim23 to affect mitochondrial transmembrane transport (55). Other research has demonstrated that at the mRNA level, α-lipoic acid, a type of antioxidant, can increase the expression of Hspa9 in both streptozotocin-induced diabetic and non-diabetic rats (58). In addition, Hspa9 can integrate with podoplanin, which is mainly expressed in podocytes, indicating an important role of Hspa9 in development of DN (59). Furthermore, ACEIs

Table II. DAVID analysis of differentially expressed proteins in the kidney cortices of untreated and fosinopril-treated OLETF rats.

Category	Term	Genes	Count	Percentage	P-value
KEGG pathway	Glycolysis/gluconeogenesis	Fbp1, Pgk1, Pdhb, Eno1	4	25	0.0005
Biological process	Generation of precursor metabolites and energy	Ndufa10, Pgk1, Pdhb, Eno1, Etfa, Mdh1	6	37.5	<0.0001
Biological process	Glycolysis	Pgk1, Pdhb, Eno1, Mdh1	4	25	<0.0001
Biological process	Glucose metabolic process	Fbp1, Pgk1, Pdhb, Eno1, Mdh1	5	31.25	<0.0001
Biological process	Monosaccharide catabolic process	Pgk1, Pdhb, Eno1, Mdh1	4	25	<0.0001
Biological process	Hexose metabolic process	Fbp1, Pgk1, Pdhb, Eno1, Mdh1	5	31.25	<0.0001
Biological process	Alcohol catabolic process	Pgk1, Pdhb, Eno1, Mdh1	4	25	0.0001
Biological process	Cellular carbohydrate catabolic process	Pgk1, Pdhb, Eno1, Mdh1	4	25	0.0001
Biological process	Monosaccharide metabolic process	Fbp1, Pgk1, Pdhb, Eno1, Mdh1	5	31.25	0.0001
Biological process	Carbohydrate catabolic process	Pgk1, Pdhb, Eno1, Mdh1	4	25	0.0001
Biological process	Pyruvate metabolic process	Fbp1, Pgk1, Pdhb	3	18.75	0.0010
Biological process	Oxidation reduction	Gpx3, Ndufa10, Pdhb, Etfa, Mdh1	5	31.25	0.0032
Biological process	Coenzyme metabolic process	Gpx3, Pdhb, Mdh1	3	18.75	0.0123
Biological process	Cofactor metabolic process	Gpx3, Pdhb, Mdh1	3	18.75	0.0192
Biological process	Gluconeogenesis	Fbp1, Pgk1	2	12.5	0.0245
Biological process	Hexose biosynthetic process	Fbp1, Pgk1	2	12.5	0.0287
Biological process	Monosaccharide biosynthetic process	Fbp1, Pgk1	2	12.5	0.0370
Biological process	Acetyl-CoA metabolic process	Pdhb, Mdh1	2	12.5	0.0401
Biological process	Alcohol biosynthetic process	Fbp1, Pgk1	2	12.5	0.0463
Biological process	Response to drug	Apoa1, Gpx3, Ndufa10	3	18.75	0.0467
Subcellular localization	Mitochondrial matrix	Echs1, Ndufa10, Pdhb, Etfa, Hspa9	5	31.25	0.0001
Subcellular localization	Mitochondrial lumen	Echs1, Ndufa10, Pdhb, Etfa, Hspa9	5	31.25	0.0001
Subcellular localization	Mitochondrion	Fahd1, Nme2, Echs1, Dpysl2, Ndufa10, Pdhb, Etfa, Mdh1, Hspa9	9	56.25	0.0001
Subcellular localization	Soluble fraction	Gpx3, Fbp1, Pgk1, Eno1, Mdh1	5	31.25	0.0006
Subcellular localization	Intracellular organelle lumen	Apoa1, Echs1, Ndufa10, Pdhb, Etfa, Hspa9	6	37.5	0.0182
Subcellular localization	Organelle lumen	Apoa1, Echs1, Ndufa10, Pdhb, Etfa, Hspa9	6	37.5	0.0210
Subcellular localization	Membrane-enclosed lumen	Apoa1, Echs1, Ndufa10, Pdhb, Etfa, Hspa9	6	37.5	0.0235
Molecular function	Magnesium ion binding	Fahd1, Nme2, Fbp1, Eno1	4	25	0.0044
Molecular function	Selenium binding	Gpx3, Selenbp1	2	12.5	0.0209
Molecular function	Hydro-lyase activity	Echs1, Eno1	2	12.5	0.0436

OLETF, Otsuka Long-Evans Tokushima Fatty; KEGG, Kyoto Encyclopedia of Genes and Genomes.

can affect the expression of Hspa9, as has been demonstrated by a study where treatment with the ACEI captopril delayed the apoptotic tube collapse of bovine retinal endothelial cells and upregulated the level of Hspa9 expression in these cells (60). Taken together, it can be further hypothesized that the oxidative stress-inhibitory or renoprotective effects of ACEIs correlate with the upregulation of Hspa9 expression.

In conclusion, the present study determined that 17 proteins were significantly changed in the FP-treated kidney cortex. The increased expression levels of Hspa9 and Gpx3 following FP treatment were confirmed by western blot analysis These identified differentially expressed proteins may not only improve understanding of the mechanism of ACEIs in OLETF rats, but may also provide potential drug targets for the treatment of DN.

Acknowledgements

Not applicable.

Funding

The present study was supported by a grant from National Natural Science Foundation of China (grant nos. 81873140, 81620108031, 81773958 and 81100518) and Universities Technology Research Project of Hebei province (grant no. QN2014013).

Availability of data and materials

The datasets used and/or analyzed during the present study are available from the corresponding author on reasonable request.

Authors' contributions

ZL, YL, HZ and PL designed the present study and wrote the manuscript. ZL and HZ performed the majority of experiments. ZP and XW performed western blotting.

Ethics approval and consent to participate

The present study was approved by the Ethics Committee of China-Japan Friendship Hospital (Beijing, China).

Patient consent for publication

Not applicable.

Competing interests

The authors declare that they have no competing interests.

References

1. Umanath K and Lewis JB: Update on diabetic nephropathy: Core curriculum 2018. Am J Kidney Dis 71: 884-895, 2018.
2. Yerram P, Karuparthi PR, Hesemann L, Horst J and Whaley-Connell A: Chronic kidney disease and cardiovascular risk. J Am Soc Hypertens 1: 178-184, 2007.
3. Botdorf J, Chaudhary K and Whaley-Connell A: Hypertension in cardiovascular and kidney disease. Cardiorenal Med 1: 183-192, 2011.
4. Hayden MR, Sowers KM, Pulakat L, Joginpally T, Krueger B, Whaley-Connell A and Sowers JR: Possible mechanisms of local tissue renin-angiotensin system activation in the cardiorenal metabolic syndrome and type 2 diabetes mellitus. Cardiorenal Med 1: 193-210, 2011.
5. Liu Z, Huang XR, Chen HY, Penninger JM and Lan HY: Loss of angiotensin-converting enzyme 2 enhances TGF-β/Smad-mediated renal fibrosis and NF-κB-driven renal inflammation in a mouse model of obstructive nephropathy. Lab Invest 92: 650-661, 2012.
6. Nistala R, Whaley-Connell A and Sowers JR: Redox control of renal function and hypertension. Antioxid Redox Signal 10: 2047-2089, 2008.
7. Kobori H, Nangaku M, Navar LG and Nishiyama A: The intrarenal renin-angiotensin system: From physiology to the pathobiology of hypertension and kidney disease. Pharmacol Rev 59: 251-287, 2007.
8. Karalliedde J and Viberti G: Evidence for renoprotection by blockade of the renin-angiotensin-aldosterone system in hypertension and diabetes. J Hum Hypertens 20: 239-253, 2006.
9. Kunz R, Friedrich C, Wolbers M and Mann JF: Meta-analysis: Effect of monotherapy and combination therapy with inhibitors of the renin angiotensin system on proteinuria in renal disease. Ann Intern Med 148: 30-48, 2008.
10. Balakumar P, Arora MK, Ganti SS, Reddy J and Singh M: Recent advances in pharmacotherapy for diabetic nephropathy: Current perspectives and future directions. Pharmacol Res 60: 24-32, 2009.
11. Magee C, Grieve DJ, Watson CJ and Brazil DP: Diabetic nephropathy: A Tangled Web to Unweave. Cardiovasc Drugs Ther 31: 579-592, 2017.
12. Brownlee M: The pathobiology of diabetic complications: A unifying mechanism. Diabetes 54: 1615-1625, 2005.
13. Kong LL, Wu H, Cui WP, Zhou WH, Luo P, Sun J, Yuan H and Miao LN: Advances in murine models of diabetic nephropathy. J Diabetes Res 2013: 797548, 2013.
14. Zhang H, Li P, Burczynski FJ, Gong Y, Choy P, Sha H and Li J: Attenuation of diabetic nephropathy in Otsuka Long-Evans Tokushima fatty (OLETF) rats with a combination of Chinese herbs (Tangshen Formula). Evid Based Complement Alternat Med 2011: 613737, 2011.
15. Kawano K, Hirashima T, Mori S, Saitoh Y, Kurosumi M and Natori T: Spontaneous long-term hyperglycemic rat with diabetic complications. Otsuka Long-Evans Tokushima Fatty (OLETF) strain. Diabetes 41: 1422-1428, 1992.
16. Council NR: Guide for the care and use of laboratory animals: Eighth edition. The National Academies Press, Washington, DC, 2011.
17. Forbes JM, Thallas V, Thomas MC, Founds HW, Burns WC, Jerums G and Cooper ME: The breakdown of preexisting advanced glycation end products is associated with reduced renal fibrosis in experimental diabetes. FASEB J 17: 1762-1764, 2003.
18. Veniant M, Heudes D, Clozel JP, Bruneval P and Menard J: Calcium blockade versus ACE inhibition in clipped and unclipped kidneys of 2K-1C rats. Kidney Int 46: 421-429, 1994.
19. Zhang PL, Rothblum LI, Han WK, Blasick TM, Potdar S and Bonventre JV: Kidney injury molecule-1 expression in transplant biopsies is a sensitive measure of cell injury. Kidney Int 73: 608-614, 2008.
20. Ramachandra Rao SP, Wassell R, Shaw MA and Sharma K: Profiling of human mesangial cell subproteomes reveals a role for calmodulin in glucose uptake. Am J Physiol Renal Physiol 292: F1182-F1189, 2007.
21. Li Z, Zhang H, Dong X, Burczynski FJ, Choy P, Yang F, Liu H, Li P and Gong Y: Proteomic profile of primary isolated rat mesangial cells in high-glucose culture condition and decreased expression of PSMA6 in renal cortex of diabetic rats. Biochem Cell Biol 88: 635-648, 2010.
22. Biron DG, Brun C, Lefevre T, Lebarbenchon C, Loxdale HD, Chevenet F, Brizard JP and Thomas F: The pitfalls of proteomics experiments without the correct use of bioinformatics tools. Proteomics 6: 5577-5596, 2006.
23. Huang da W, Sherman BT and Lempicki RA: Systematic and integrative analysis of large gene lists using DAVID bioinformatics resources. Nat Protoc 4: 44-57, 2009.
24. Johnson SA and Spurney RF: Twenty years after ACEIs and ARBs: Emerging treatment strategies for diabetic nephropathy. Am J Physiol Renal Physiol 309: F807-F820, 2015.
25. Hsu FY, Lin FJ, Ou HT, Huang SH and Wang CC: Renoprotective effect of angiotensin-converting enzyme inhibitors and angiotensin II receptor blockers in diabetic patients with proteinuria. Kidney Blood Press Res 42: 358-368, 2017.
26. Shani M, Vinker S and Feldman L: End-stage renal disease and adherence to angiotensin-converting enzyme inhibitors and angiotensin receptor blockers among patients with diabetes. J Clin Hypertens (Greenwich) 19: 627-631, 2017.
27. Rossing K, Jacobsen P, Pietraszek L and Parving HH: Renoprotective effects of adding angiotensin II receptor blocker to maximal recommended doses of ACE inhibitor in diabetic nephropathy: A randomized double-blind crossover trial. Diabetes Care 26: 2268-2274, 2003.
28. Bakris GL and Weir MR: Angiotensin-converting enzyme inhibitor-associated elevations in serum creatinine: Is this a cause for concern? Arch Intern Med 160: 685-693, 2000.
29. van de Ven PJ, Beutler JJ, Kaatee R, Beek FJ, Mali WP and Koomans HA: Angiotensin converting enzyme inhibitor-induced renal dysfunction in atherosclerotic renovascular disease. Kidney Int 53: 986-993, 1998.
30. Chapman AB, Gabow PA and Schrier RW: Reversible renal failure associated with angiotensin-converting enzyme inhibitors in polycystic kidney disease. Ann Intern Med 115: 769-773, 1991.
31. Singhvi SM, Duchin KL, Morrison RA, Willard DA, Everett DW and Frantz M: Disposition of fosinopril sodium in healthy subjects. Br J Clin Pharmacol 25: 9-15, 1988.

32. Lambers Heerspink HJ and Gansevoort RT: Albuminuria is an appropriate therapeutic target in patients with CKD: The pro view. Clin J Am Soc Nephrol 10: 1079-1088, 2015.
33. Diwakar R, Pearson AL, Colville-Nash P, Brunskill NJ and Dockrell ME: The role played by endocytosis in albumin-induced secretion of TGF-beta1 by proximal tubular epithelial cells. Am J Physiol Renal Physiol 292: F1464-F1470, 2007.
34. Moon JY, Tanimoto M, Gohda T, Hagiwara S, Yamazaki T, Ohara I, Murakoshi M, Aoki T, Ishikawa Y, Lee SH, *et al*: Attenuating effect of angiotensin-(1-7) on angiotensin II-mediated NAD(P)H oxidase activation in type 2 diabetic nephropathy of KK-A(y)/Ta mice. Am J Physiol Renal Physiol 300: F1271-F1282, 2011.
35. Stephan JP, Mao W, Filvaroff E, Cai L, Rabkin R and Pan G: Albumin stimulates the accumulation of extracellular matrix in renal tubular epithelial cells. Am J Nephrol 24: 14-19, 2004.
36. Wolf G, Schroeder R, Ziyadeh FN and Stahl RA: Albumin up-regulates the type II transforming growth factor-beta receptor in cultured proximal tubular cells. Kidney Int 66: 1849-1858, 2004.
37. Burton C and Harris KP: The role of proteinuria in the progression of chronic renal failure. Am J Kidney Dis 27: 765-775, 1996.
38. Behne D and Kyriakopoulos A: Mammalian selenium-containing proteins. Annu Rev Nutr 21: 453-473, 2001.
39. Haung W, Koralewska-Makar A, Bauer B and Akesson B: Extracellular glutathione peroxidase and ascorbic acid in aqueous humor and serum of patients operated on for cataract. Clin Chim Acta 261: 117-130, 1997.
40. Whitin JC, Bhamre S, Tham DM and Cohen HJ: Extracellular glutathione peroxidase is secreted basolaterally by human renal proximal tubule cells. Am J Physiol Renal Physiol 283: F20-F28, 2002.
41. Kang SW, Natarajan R, Shahed A, Nast CC, LaPage J, Mundel P, Kashtan C and Adler SG: Role of 12-lipoxygenase in the stimulation of p38 mitogen-activated protein kinase and collagen alpha5(IV) in experimental diabetic nephropathy and in glucose-stimulated podocytes. J Am Soc Nephrol 14: 3178-3187, 2003.
42. de Cavanagh EM, Inserra F, Toblli J, Stella I, Fraga CG and Ferder L: Enalapril attenuates oxidative stress in diabetic rats. Hypertension 38: 1130-1136, 2001.
43. Ogawa S, Mori T, Nako K, Kato T, Takeuchi K and Ito S: Angiotensin II type 1 receptor blockers reduce urinary oxidative stress markers in hypertensive diabetic nephropathy. Hypertension 47: 699-705, 2006.
44. Sonta T, Inoguchi T, Matsumoto S, Yasukawa K, Inuo M, Tsubouchi H, Sonoda N, Kobayashi K, Utsumi H and Nawata H: In vivo imaging of oxidative stress in the kidney of diabetic mice and its normalization by angiotensin II type 1 receptor blocker. Biochem Biophys Res Commun 330: 415-422, 2005.
45. Ishizawa K, Izawa-Ishizawa Y, Dorjsuren N, Miki E, Kihira Y, Ikeda Y, Hamano S, Kawazoe K, Minakuchi K, Tomita S, *et al*: Angiotensin II receptor blocker attenuates PDGF-induced mesangial cell migration in a receptor-independent manner. Nephrol Dial Transplant 25: 364-372, 2010.
46. Lv J, Jia R, Yang D, Zhu J and Ding G: Candesartan attenuates Angiotensin II-induced mesangial cell apoptosis via TLR4/MyD88 pathway. Biochem Biophys Res Commun 380: 81-86, 2009.
47. Park SJ, Lee BH and Kim DJ: Identification of proteins that interact with podocin using the yeast 2-hybrid system. Yonsei Med J 50: 273-279, 2009.
48. Morito N, Yoh K, Ojima M, Okamura M, Nakamura M, Hamada M, Shimohata H, Moriguchi T, Yamagata K and Takahashi S: Overexpression of Mafb in podocytes protects against diabetic nephropathy. J Am Soc Nephrol 25: 2546-2557, 2014.
49. Chiu YW, Kuo MC, Kuo HT, Chang JM, Guh JY, Lai YH and Chen HC: Alterations of glomerular and extracellular levels of glutathione peroxidase in patients and experimental rats with diabetic nephropathy. J Lab Clin Med 145: 181-186, 2005.
50. Fan QL, Yang G, Liu XD, Ma JF, Feng JM, Jiang Y and Wang LN: Effect of losartan on the glomerular protein expression profile of type 2 diabetic KKAy mice. J Nephrol 26: 517-526, 2013.
51. Kaul SC, Deocaris CC and Wadhwa R: Three faces of mortalin: A housekeeper, guardian and killer. Exp Gerontol 42: 263-274, 2007.
52. Wadhwa R, Ryu J, Ahn HM, Saxena N, Chaudhary A, Yun CO and Kaul SC: Functional significance of point mutations in stress chaperone mortalin and their relevance to Parkinson disease. J Biol Chem 290: 8447-8456, 2015.
53. Deocaris CC, Widodo N, Shrestha BG, Kaur K, Ohtaka M, Yamasaki K, Kaul SC and Wadhwa R: Mortalin sensitizes human cancer cells to MKT-077-induced senescence. Cancer Lett 252: 259-269, 2007.
54. Liu Y, Liu W, Song XD and Zuo J: Effect of GRP75/mthsp70/PBP74/mortalin overexpression on intracellular ATP level, mitochondrial membrane potential and ROS accumulation following glucose deprivation in PC12 cells. Mol Cell Biochem 268: 45-51, 2005.
55. Matsuoka T, Wada J, Hashimoto I, Zhang Y, Eguchi J, Ogawa N, Shikata K, Kanwar YS and Makino H: Gene delivery of Tim44 reduces mitochondrial superoxide production and ameliorates neointimal proliferation of injured carotid artery in diabetic rats. Diabetes 54: 2882-2890, 2005.
56. Lv Y, Li Y, Zhang D, Zhang A, Guo W and Zhu S: HMGB1-induced asthmatic airway inflammation through GRP75-mediated enhancement of ER-mitochondrial Ca^{2+} transfer and ROS increased. J Cell Biochem 119: 4205-4215, 2018.
57. Honrath B, Metz I, Bendridi N, Rieusset J, Culmsee C and Dolga AM: Glucose-regulated protein 75 determines ER-mitochondrial coupling and sensitivity to oxidative stress in neuronal cells. Cell Death Discov 3: 17076, 2017.
58. Oksala NK, Lappalainen J, Laaksonen DE, Khanna S, Kaarniranta K, Sen CK and Atalay M: Alpha-lipoic Acid modulates heat shock factor-1 expression in streptozotocin-induced diabetic rat kidney. Antioxid Redox Signal 9: 497-506, 2007.
59. Tsuneki M, Maruyama S, Yamazaki M, Xu B, Essa A, Abé T, Babkair H, Cheng J, Yamamoto T and Saku T: Extracellular heat shock protein A9 is a novel interaction partner of podoplanin in oral squamous cell carcinoma cells. Biochem Biophys Res Commun 434: 124-130, 2013.
60. Hamdi HK and Castellon R: ACE inhibition actively promotes cell survival by altering gene expression. Biochem Biophys Res Commun 310: 1227-1235, 2003.